Modeling Laser Bandwidth for OPC Applications

Christian Zuniga[a], Kostas Adam[a], Michael Lam[a], Ivan Lalovic[b], Peter De Bisschop[c]

[a]Mentor Graphics Corp., 1001 Ridder Park Dr. San Jose Ca USA
[b]Cymer, Inc., 17075 Thornmint Court, San Diego, CA USA
[c]IMEC, Kapeldreef 75, Leuven 3001, Belgium

ABSTRACT

With the push toward 32 nm half-pitch, OPC models will need to account for a wider range of sources of imaging variability in order to meet the CD budget requirements. The effects of chromatic aberration on imaging have been a recent area of interest but little work has been done to include this effect in OPC models. Chromatic aberrations in the optical system give rise to a blurring of the intensity distribution in the imaging plane even for highly line-narrowed immersion laser sources. The resulting focus blur can introduce a feature-dependent CD bias of several nanometers. Usually, the empirical components of the resist model can reduce or completely compensate for this imaging effect. However, it is not well known if including a more physical image model over a large range of laser bandwidth conditions will improve the OPC accuracy or process-variability robustness.

This study demonstrates the correlation of physical laser bandwidth perturbations with perturbations of the optical model in Calibre. The laser bandwidth is experimentally perturbed to obtain several sets of CD measurements for different bandwidths. These are then used in model calibration with the corresponding perturbation in the optical model. Finally, we quantify the improvement in model accuracy obtained when including an input of laser bandwidth.

Keywords: laser bandwidth, laser spectrum, modeling, focus blur, chromatic aberration

1. INTRODUCTION

As the industry moves toward the 32 and 22 nm nodes, OPC models will have to incorporate several additional sources of linewidth variation to satisfy the tighter tolerance requirements. It is well known that the finite laser bandwidth in modern 193 nm systems causes the energy in the focus plane to become spread out, an effect commonly known as focus blur [1] [2] [3]. It has also been shown previously that structures which are more sensitive to defocus will have higher sensitivity to variations of the laser bandwidth [4][5]. The resulting effect of changes in laser bandwidth is a feature-dependent bias that can be as large as several nanometers for the focus-sensitive isolated or semi-isolated structures if the bandwidth variation is not actively stabilized.

One of the objectives of this work is to quantify the OPC improvement from incorporating a laser bandwidth input into the optical model in Calibre. We calibrated OPC models with line/space measurements obtained at different settings of laser bandwidth and compared the accuracy between models including information about the laser bandwidth and models that did not include it. Although Calibre allows the option of optimizing (calibrating) the laser bandwidth, the resulting parameters may not reflect the physical width or shape of the laser spectrum. We preferred to build the optical model by fitting the actual laser spectrum and tested the improvement in accuracy when using the more physical imaging model. We first used fixed resist models to quantify the ability of the OPC model to track changes in the laser bandwidth. This test may also prove useful when there is a need to transport a model to data from a different scanner or to data from the same scanner taken at different points in its lifetime since the laser bandwidths or the lens chromatic aberrations can be different. We then optimized the resist models separately for each bandwidth setting and tested the model improvement at a given setting.

Optical Microlithography XXII, edited by Harry J. Levinson, Mircea V. Dusa, Proc. of SPIE Vol. 7274,
72741O · © 2009 SPIE · CCC code: 0277-786X/09/$18 · doi: 10.1117/12.813869

The rest of the paper is organized as follows. In section 2 we first review the modeling principles for including finite laser bandwidth and/or focus blur. Section 3 is the main section describing the model calibration results over the range of laser bandwidth settings. Section 3.1 provides an overview of the experimental data. Section 3.2 describes the optical model setup and section 3.3 describes the estimation of the longitudinal chromatic aberration (LCA) parameter. Finally section 3.4 describes the results with fixed resist models and section 3.5 describes the results with variable resist models.

2. LASER BANDWIDTH MODELING

The effect of the laser spectrum on the image intensity is modeled as a weighted superposition of images over a range of defocus values. The range of defocus values is determined from the lens design constant, $df / d\lambda$, which relates the change in focus (df) resulting from a wavelength offset (dλ) [6]. This parameter is commonly referred to as the longitudinal chromatic aberration or LCA. The LCA is usually in the range of 200-500 nm/pm for modern 193 nm scanners [1]. The weights are obtained from an analytic distribution that models the laser spectra such as the modified Lorentzian distribution or from spectrophotometry of the laser output. Equation 1 gives the final normalized form of the intensity where f_0 is the nominal focus position and P(f) is a distribution function obtained via measurements or analytical approximation. This formulation has the advantage that the function P(f) can also be generalized to incorporate other sources of focus blur such as stage vibrations or stage tilt, all of which may exhibit differing distribution functions.

$$I(x,y,z;f_0,P(f)) = \int_{-\infty}^{\infty} I(x,y,z;f_0 - f)P(f - f_0)df \Big/ \int_{-\infty}^{\infty} P(f - f_0)df \tag{1}$$

Two commonly used functions to approximate focus blur from non-monochromatic lasers are the modified Lorentzian and Gaussian functions. Equation 2 shows the form of the modified Lorentzian function. The modified Lorentzian distribution is characterized by two parameters, the full-width-at-half-maximum, or FWHM, and exponent n. The FWHM gives a measure of the width of the distribution at 50% intensity and n describes the decay of the tails. The FWHM of the focus blur distribution is linearly related to the FWHM of the laser spectrum by the LCA so $FWHM_f$ = LCA x $FWHM_\lambda$.

$$P_{ML}(f - f_0) = \frac{FWHM_f^n}{|2(f - f_0)|^n + FWHM_f^n} \tag{2}$$

However, it has been shown that the modified Lorentzian does not fit the laser spectrum well at the tails [3]. It has also been found that, instead of FWHM, a more reliable measure of the imaging effects of the laser bandwidth is the E95 metric [7], where E95 is the bandwidth that contains 95% of the laser energy. In this paper we used the E95 to quantify the laser bandwidth and fitted the analytic functions to the spectrum.

The Gaussian function is also commonly used to model the laser spectrum. It can sometimes fit the spectrum better than the modified Lorentzian in the center region of the spectrum [8]. It also does not fit the tails of the spectrum well, however. It is characterized by a single parameter σ_λ. The σ_λ that best describes the spectrum has been found to be σ_λ = E95/4. This estimate follows from the fact that for a Gaussian, 4σ contains approximately 95% of the energy. The corresponding focus blur value is σ_f = LCA x σ_λ.

The analytic functions do not capture the tails of the spectrum accurately as well as any asymmetries present. An actual laser spectrum can also be used to obtain the intensity using a full set of measured samples obtained by high-accuracy spectrophotometry. The best modeling solution is to use the measured laser spectrum in the optical model, but in practice there are three reasons that have prevented widespread adoption of such a scenario: 1) the extra step of measuring the laser spectrum, 2) the fact that such spectral data are typically considered proprietary by the laser manufacturer and are not easily obtainable and, 3) the fact that the LCA parameter is also considered proprietary by the scanner manufacturer and, without it, the end-user is still forced to have the extra step of fitting the focus blur distribution function of Eq. (1) to CD measurements. When a focus blur distribution function is used - either analytical or measured – the optical model generation involves computation of the TCC matrix over multiple focus conditions, such that the numerical integration of Eq. (1) is performed to acceptable accuracy. The optical model genera ration will be slower approximately proportionally to the number of focus conditions used to perform the integration. The number of focus conditions needed

to perform the integration to acceptable accuracy for typical laser spectra ranges between 5 and 20. It must be stressed that the OPC runtime once the optical model is generated does not depend on whether the optical model contains any focus blur or not, and consequently, if focus blur from non-zero laser bandwidth is modeled, the OPC runtime does not depend on the number of focus conditions used to carry out the integration of Eq. (1).

3. MODEL CALIBRATION WITH LASER BANDWIDTH

3.1 Experimental Data

The experimental data set consisted of five sets of process window data with five corresponding values of laser bandwidth, as measured by E95. The data was collected using an ASML 1700i scanner and a XLA 360 laser from Cymer. In these experiments, the laser bandwidth was varied over a range which was wider than the typical variation of this laser model running in production, using a combination of modified operating parameters and other experimental techniques. More recent laser systems, such as the XLR 500i or XLR 600i on >1.3NA immersion systems, feature an adjustable line-narrowing module, which allows changing the laser bandwidth over a range of set-points without impact on other performance parameters. The photoresist CD features consisted of 30 line/space patterns ranging in pitch from 100 to 400 nm with a variable mask CD ranging from 44 nm at pitch 100 nm to 106 nm at pitch 400 nm. The mask CD varied to decrease the variation of the printed CDs through pitch. Table 1 summarizes the experimental conditions. Figure 1 shows the CD measurements through pitch at one process window condition. As expected, increasing E95 bandwidth causes the more isolated lines to print smaller. The dense lines remain largely unaffected.

Table 1 Summary of experimental process conditions

Parameter	Values
E95	0.222, 0.31,0.381,0.41,0.48 pm
NA	1.2
Dose	23.0-25.0 in steps of 0.5 mJ/cm^2
Focus	-90-110 in steps of 10 nm
Illumination	cQuad20 0.96/0.6
Polarization	XY
Film Stack	Resist TOK TArF-Pi6-001-ME 120 nm on ARC29SR 95 nm, Substrate Si

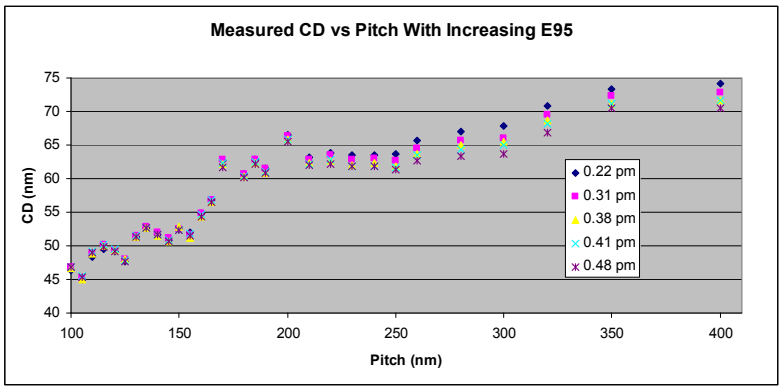

Figure 1 shows the measured CD vs. pitch for the 5 E95 values used. The focus was 10 nm and dose was 24.5 mJ/cm^2.

The modified Lorentzian values of the laser spectrum were obtained by fitting to laser spectra obtained from factory measurements of the Cymer XLA 360 lasers using the method of least squares. Table 2 shows the resulting FWHM and n values.

Table 2 Modified Lorentzian values obtained by fitting to the laser spectrum.

E95 (pm)	FWHM (pm)	n
0.222	0.102	3.5
0.309	0.142	3.4
0.381	0.176	3.4
0.41	0.195	3.3
0.48	0.222	3.3

3.2 Optical Model Setup

We used the optical settings in Table 1 to build the optical model in Calibre. We kept 30 optical kernels with an optical diameter of 1.5 μm to have good balance between accuracy and speed. We also obtained a fit to the measured illuminator to have a symmetrical source model. Two parameters in the optical model that are not initially apparent are the beamfocus and defocus_start. Beamfocus refers to the location of best image focus without any film, and defocus_start refers to the depth within the resist where the intensity is sampled to obtain the CD. Both are measured from the top of the film stack and affect the location of best CD focus. The simulated best CD focus and experimental best CD focus must be properly matched to obtain a good model.

These two parameters could also be optimized but in the interest of forming a more physical optical model, we used a simple method to determine beamfocus given defocus_start. Analyzing the imaging equations for three-beam interference, a matched substrate, and a threshold resist model gives an approximate relation between defocus start and beamfocus. This approach follows the techniques described in [9][10] and is expected to be published as well. The simplest relation is given by Equation 3.

$$beamfocus = \frac{n_i}{n_r} defocus\_start \tag{3}$$

The parameters n_i and n_r refer to the real part of the index of refraction of the immersion medium and the resist, respectively. Equation 3 does not independently specify what defocus_start should be but it does specify what beamfocus should be if defocus_start is fixed to obtain the maximum/minimum CD at zero defocus. The intensity is attenuated further into the resist so changing defocus_ start is comparable to changing the threshold. To first order, defocus_start does not participate in specifying the best simulated CD focus. Since the CDs are usually taken to be at the bottom of the resist, we placed defocus_start close to the bottom at 110 nm. The corresponding beamfocus value using Equation 3 is 95 nm. Figure 2 shows a simulated CD vs. defocus curve for feature v106p400 (pitch 400 nm) using these values. Beamfocus corresponds to zero defocus in the plot. As the figure shows, the maximum CD does not occur at zero defocus as Equation 2 indicates but at ~ -10 nm. Adding this offset to the estimate gives a beamfocus of 85 nm. Figure 2 also shows that with this new beamfocus, the CD attains its maximum value at zero defocus. Equation 3 has been found to hold well for other defocus_start values and serves as a guide in determining these parameters.

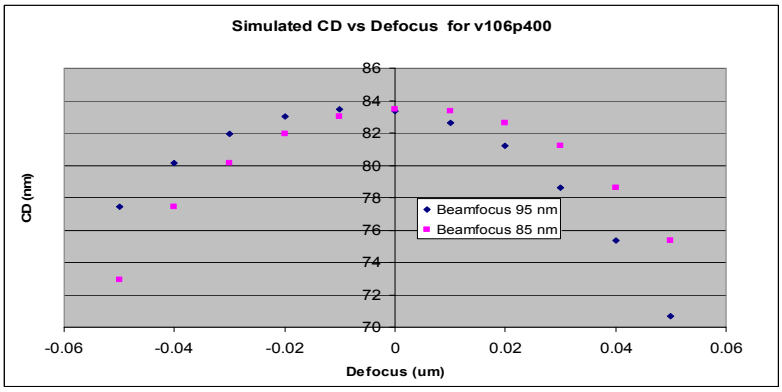

Figure 2 CD vs. defocus curves for feature v106p400 (pitch 400 nm) with the same defocus_start of 110 nm but different beamfocus values.

In the experimental data, the CD attains its maximum value at ~10 nm defocus. The data can be shifted to move the maximum CD to zero defocus or an offset can be added to beamfocus. Adding the offset to the estimated beamfocus gives a new beamfocus of 75 nm. This new value of beamfocus now corresponds to zero defocus. At 10 nm defocus, beamfocus becomes 85 nm, shifting the focus value of maximum CD to 10 nm defocus and matching the experimental best focus. The presence of the laser bandwidth is not expected to alter the best CD focus [4] so we compared the models with and without laser bandwidth using the same beamfocus and defocus start settings.

3.3 Estimating LCA

The value of LCA is normally considered proprietary by the exposure system manufacturers and was not known for this experiment. For this reason it will also be referred to in this paper as LCA_est. It can however be directly measured or estimated from the measured data. From reference [4], it is expected that the laser spectrum gives a change in CD according to Equation 4, shown below. $E95_1$ refers to the lowest bandwidth setting in Table 1 and $E95_k$ increases as the index k increases. The parameter Q_F is the quadratic focus sensitivity and can be obtained by fitting a quadratic to a measured CD vs. defocus curve. We used the feature at pitch 400 nm to obtain an estimate of Q_F of -2.2 $\mu m/\mu m^2$. Solving for the LCA in Equation 4 for each change of E95 gives an estimate of LCA of LCA_est ±50 nm/pm that is within the expected range of 200-500 nm/pm. To further narrow down the estimate, we tried a few values in this estimated range. Figure 3 shows the resulting simulated CDs obtained with three different values of LCA from the estimated range and the fitted modified Lorentzians in Table 2. We used a constant threshold model (CTR model) calibrated to the lowest bandwidth setting. Using LCA_est gives the lowest errors and gives a good initial value to begin with. We followed the same procedure when using the Gaussian focus blur. Through several model iterations, the value could be further refined if greater accuracy is desired. Alternatively, tool operators can measure this value from their exposure system by changing the wavelength set-point and determining the image best focus.

$$\Delta CD_k \approx 0.056(LCA^2)Q_F(E95_k^2 - E95_1^2) \qquad k = 2..5 \tag{4}$$

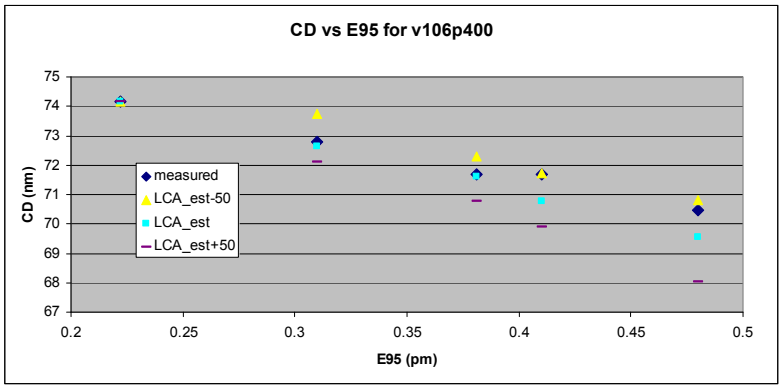

Figure 3 Measured and simulated CD for feature at pitch 400, at focus 10 nm dose 24 mJ/cm^2, using a CTR model. The threshold was calibrated for the CD with the lowest E95 setting. The figure shows the change in CD at 3 LCA values with LCA_est being the best one and at ± 50 nm/pm.

3.4 Model Calibration with Fixed Resist Models and Varying Laser Bandwidth.

In order to confirm that the modified Lorentzian focus blur can track changes in E95, we used fixed resist models. We obtained the resist model by using the data set obtained with the lowest E95 setting to calibrate the resist model. We then applied this resist model to the remaining four bandwidth settings. As Equation 4 shows, the CD is a quadratic function of E95 so the effects at the lowest E95 setting are less pronounced. This is the simplest and fastest method of obtaining the resist model and serves as a quick verification of the estimated LCA value. It has the disadvantage that the resist model is still absorbing some laser bandwidth effects. A more accurate approach would be to include the laser bandwidth for the lowest setting. We used this approach when modeling larger data sets. We also used resist models of increasing complexity as needed to keep the errors low, or as the pitch, dose, and focus range was increased. We started from a threshold model, moved on to a double Gaussian model, and finally to higher compact models (CM1 modelforms) for the entire through pitch process window data. Figure 3 in the previous section shows an example result with a threshold model for one pitch at one process window condition. As the figure shows, adding the expected amount of focus blur to the model compensates for the changes in E95.

As the pitch range increases, it becomes necessary to use a more sophisticated resist model to lower the through-pitch modeling error. The double Gaussian resist model has been shown to be a good model through pitch [11][12][13]. It extends the threshold model to account for acid and base diffusion in the resist and has the form given by Equation 5.

$$c_0(I \otimes G_0) + c_1(I \otimes G_1) = T \tag{5}$$

The image intensity I is convolved with two Gaussians G_0 and G_1 and the resulting images are weighted and added together. The CD is extracted by thresholding this final image.

Repeating the calibration of the data with the lowest bandwidth setting with a double Gaussian resist model gives an RMS error of ~1.65 nm. Keeping this resulting resist model fixed and changing only the focus blur values in the optical models keeps the RMS error around the same value for the through-pitch data as E95 increases. Table 3 shows the resulting verification errors for the four remaining through-pitch data sets (30 points per set) as a function of laser bandwidth at one process window condition. Figure 4 shows an example result in the case of the highest bandwidth setting. The monochromatic errors in this table refer to the errors for the model which does not include a laser bandwidth input. The simulated CDs have the same value for all E95 settings. As expected, the errors increase as E95 increases for the monochromatic model. The RMS errors for the two models with laser bandwidth input are roughly of the same magnitude, indicating the addition of the expected focus blur is tracking well the changes in E95. The models with laser bandwidth input offer a maximum improvement of about a 0.5 nm RMS over the monochromatic model. The maximum error is also reduced by including the laser bandwidth and gives about a 1.6 nm maximum improvement. Figure 4 shows

that much of the improvement in error comes from better matching of the more isolated lines. The Gaussian focus blur gives a lower RMS error but a larger maximum error than the modified Lorentzian. Repeating the same experiment by extracting the resist model at a different E95 setting also shows that the models with laser bandwidth input are able to track changes in E95.

Ideally, the errors in the models with laser bandwidth should stay the same and further refinements of the model are expected to do this. The accuracy of the value of LCA could be further improved and other parameters in the optical model such as beamfocus can be further refined. However, random noise in the calibration data also contributes to an increasing error at the larger E95 values and a more accurate model may require calibration with data at more than one E95 setting.

Table 3 CD errors obtained with and without the addition of laser bandwidth as E95 increases.

E95 (pm)	**Monochromatic Model Errors (nm)**	**Modified Lorentzian Model Errors (nm)**	**Gaussian Model Errors (nm)**
0.222	RMS 1.65, MAX 5.85	RMS 1.70, MAX 6.1	RMS 1.70, MAX 6.08
0.31	RMS 1.79, MAX 5.82	RMS 1.73, MAX 5.29	RMS 1.71, MAX 5.38
0.381	RMS 2.00, MAX 6.19	RMS 1.73, MAX 5.27	RMS 1.71, MAX 5.43
0.41	RMS 2.11, MAX 6.06	RMS 1.89, MAX 4.85	RMS 1.78, MAX 5.14
0.48	RMS 2.45, MAX 6.35	RMS 2.04, MAX 4.70	RMS 1.85, MAX 5.02

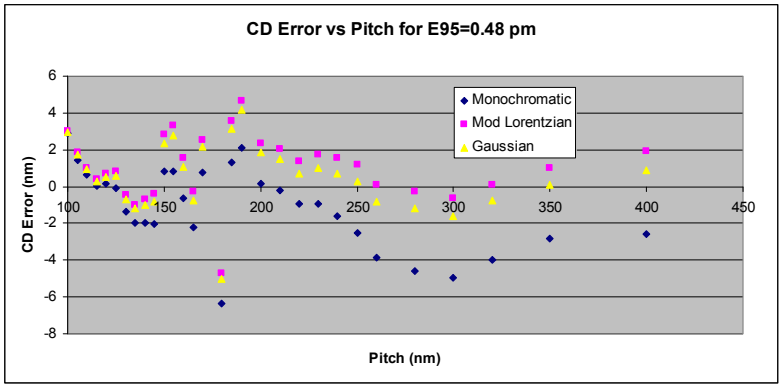

Figure 4 CD error vs. pitch for the setting E95=0.48pm. The model which includes the laser bandwidth input is able to bring the isolated lines down, better matching the measured values.

3.5 Calibration with Variable Resist Models and a Fixed Laser Bandwidth

The previous section showed that a focus blur input using either the modified Lorentzian or the Gaussian for the laser bandwidth can track changes in E95. Usually, experimentally measured CD data will only be available at one E95 setting. Improvements in laser stability and particularly active bandwidth stabilization technology in the latest laser systems minimize the variations in E95. Therefore it becomes necessary to optimize the resist model with a given E95 setting. Models with no laser bandwidth input have been acceptable for larger process nodes (65 nm and above) but may no longer be sufficient. Without the focus blur input, the resist model compensates for the presence of the laser bandwidth. The model may still achieve a low calibration error but lead to poorer prediction results. This section compares the accuracy of monochromatic models with a more accurate imaging model with a laser bandwidth input. We tested the model accuracy by verifying them with data not present in the calibration at different focus and dose

conditions. As in the previous section, we used more sophisticated resist models as we increased the range in pitch, focus, and dose of the calibration data.

As a simple example, we calibrated a threshold model at one focus condition and observed the model predictability through dose. Equation 4 shows the change in CD depends on the factor Q_F which in turn depends on dose. For the isolated lines with a downward curvature, Q_F decreases as dose decreases. The change in CD caused by the laser bandwidth should be less for the lowest doses. Studying the measured data revealed a slightly lower change in CD for the lowest dose compared to the highest. A monochromatic model that did not include CDs at the lowest doses should not be able to account for this difference. We tested this hypothesis by using two out of the five dose conditions (24 and 25 mJ/cm^2) to find the thresholds for one isolated pitch and verified the remaining three dose conditions. Figure 5 shows the results for the lowest E95 setting. As the dose decreases, the CD error increases but the maximum error remains less than 1 nm. Usually this is good enough accuracy and it may not be necessary to include the laser bandwidth. Figure 6 shows the results for the case with E95=0.41 pm. The maximum error for the monochromatic model reaches 1.8 nm. Calibrating the threshold with the corresponding focus blur present brings the maximum error down to 1.1 nm. Figure 6 shows that adding the expected focus blur gives simulated CDs closer to the measured CDs. The threshold calibrated with the expected focus blur input is better able to predict through a wider range of dose. This example suggests that adding the laser bandwidth can give a more accurate model but may only be necessary at higher E95 values.

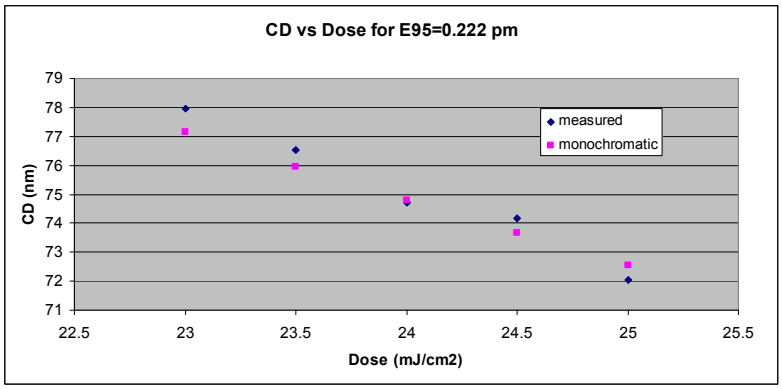

Figure 5 CD vs. dose for E95=0.22 pm at focus 0.01 nm (best focus). The threshold was calibrated to doses 24 and 25 mJ/cm^2 and used to verify the remaining three doses.

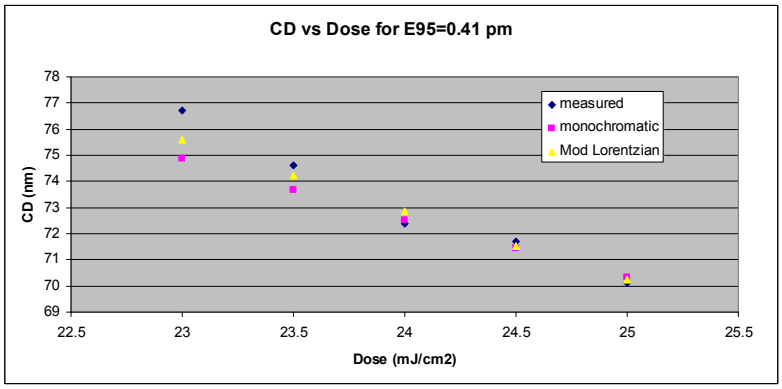

Figure 6 CD vs. dose for E95=0.41 pm at focus 0.01 nm (best focus). The threshold was calibrated to doses 24 and 25 mJ/cm^2 and used to verify the remaining three doses. The mod Lorentzian model used the expected amount of focus blur.

Repeating the experiment with a double Gaussian model and with through pitch data at one focus condition did not reveal an improvement with laser bandwidth for any of the five bandwidth settings. Both models had similar accuracy. The empirical components of the resist model were able to adequately compensate for the presence of the laser bandwidth. Possibly the resist model was able to capture information about the laser bandwidth effect on the CDs by matching the correction needed to calibrate both dense and isolated lines simultaneously.

Moving on to the entire through pitch process window data did reveal better accuracy with the addition of laser bandwidth but mostly at the highest bandwidth conditions. In this case we used modelform 21 to maintain low modeling errors [14]. Modelform 21 extends the double Gaussian model to include other effects like truncation, slope and curvature. We calibrated the models with seven process window conditions, each with approximately 30 through pitch measurements. The seven conditions had defocus values in the range -40 to 40 nm. All the models had a comparable calibration error of ~1.8 nm RMS. Verifying on ~2100 data points gave the errors shown in Table 4 for the highest bandwidth case. Adding the expected focus blur can improve the model by about 0.15 nm RMS. The maximum error was not improved however. Figures 7 and 8 show the RMS errors for each pitch for the two highest bandwidth settings. The figures show that much of the improvement comes from lower errors at the highest pitches. This is a consistent result since the laser bandwidth has a greater impact on more isolated lines. Adding the expected focus blur using either the modified Lorentzian or a Gaussian input gave a more accurate process window model.

Table 4 Errors with and without laser bandwidth for E95 = 0.48 pm.

Errors (nm)	Monochromatic	Mod Lorentzian	Gaussian
RMS	2.40	2.25	2.23
MAX	20.9	26.5	27.4

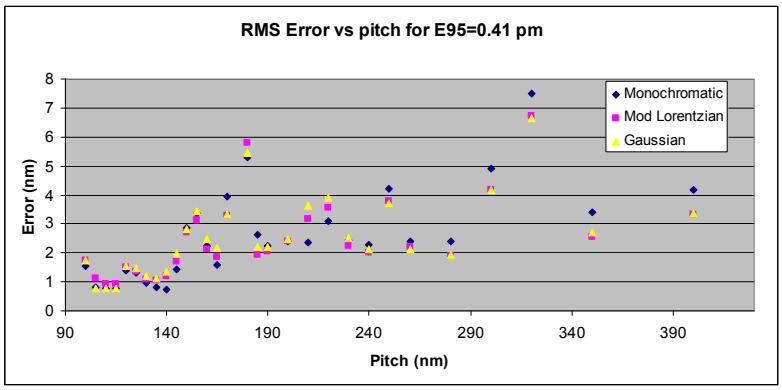

Figure 7 RMS error vs. pitch for the setting E95=0.41 pm for three models.

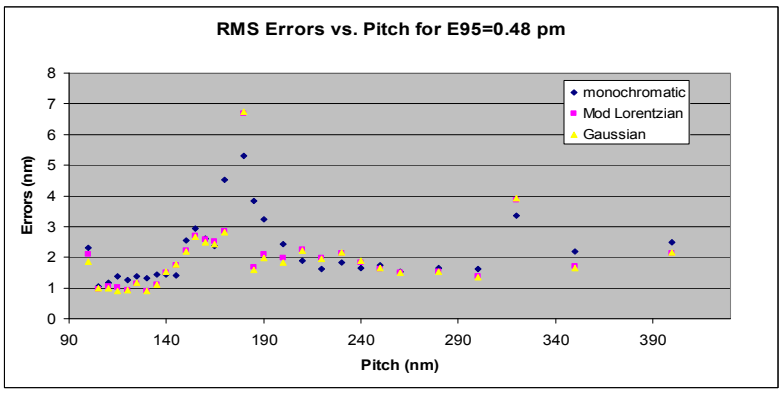

Figure 8 RMS error vs. pitch for the setting E95=0.48 pm for three models.

4. SUMMARY

In this paper, we explored how much an OPC model is improved by incorporating the expected focus blur caused by the laser bandwidth. We first estimated the value of the longitudinal chromatic aberration or LCA, a value that has a great impact on the subsequent modeling steps. Then we decoupled the resist model by calibrating it with the lowest bandwidth setting. With the resist model fixed, the optical model tracks the changes in the laser spectrum well. There is no clear advantage between the modified Lorentzian and Gaussian bandwidth models except that the Gaussian can be obtained from a much simpler estimating procedure.

Treating each bandwidth data set independently revealed an improvement when using the laser bandwidth in process window regions outside of the calibration region. The RMS error was lowered by up to 0.15 nm for the largest E95 setting. This result confirms the expectation that using a more physical model has greater predictive abilities. There was no clear improvement at the lowest bandwidth settings. The laser bandwidth effect may be embedded in other imaging and resist effects in addition to random variations that also need to be properly accounted for. Using a wider range of features may reveal a clearer advantage in using the laser bandwidth [15]. An actual laser spectrum may also give a more accurate model. Unfortunately the model calibration time increases when using the focus blur and it may not be practical to use the actual spectrum.

REFERENCES

[1] Brunner, Corliss, Butt, Wiltshire, and Ausschnitt "Laser bandwidth and other sources of focus blur in lithography" Proc. of SPIE Vol. 6154 2006, 61540V-1

[2] Huggins, Tsuyoshi, Ong, Rafac, Treadway, Choudhary, Kudo, Hirukawa, Renwick and Farrar "Effects of laser bandwidth on OPE in a modern lithography tool" Proc. of SPIE 2006 Vol. 6154, 61540Z-1

[3] Lalovic, Kritsun, McGowan, Bendik, Smith, and Farrar " Defining a physically accurate laser bandwidth input for optical proximity correction (OPC) and modeling" Proc. of SPIE vol. 7122 (2008) 71221R

[4] De Bisschop, Lalovic and Trintchouk "Impact of finite laser bandwidth on the critical dimension of L/S structures" J. Micro/Nanolith MEMS MOEMS 7(3) 033001 (Jul-Sep 2008)

[5] Yoshimochi, Uchiyama, Tamura, Theeuwes, Peeters, van der Laan, Bakker, Morisaki, and Oga "Study of iso-dense Bias sensitivity to laser spectral shape at the 45 nm node" Proc. of SPIE Vol. 6520 (2007) 652011-1

[6] Terry, Lalovic, Wells, and Smith "Behavior of lens aberrations as a function of wavelength on KrF and ArF Lithography Scanners" Proc. of SPIE Vol. 4346 (2001) pp. 15-24

[7] Kroyan, Lalovic, Farrar "Effects of 95% Integral vs. FWHM Bandwidth Specifications on Lithographic Imaging" Proc. of SPIE Vol. 4346 (2001) pp. 1244-1253

[8] Lalovic, Kritsun, Bendik, Smith, Sallee, and Farrar "Fast and accurate laser bandwidth modeling of optical proximity effects" BACUS Photomask 2007, Sep17-21

[9] Mack, *Fundamental Principles of Optical Lithography* John Wily & Sons Copyright 2007

[10] Gu, *Advanced Optical Imaging Theory* Springer Copyright 2000

[11] Brunner, Fonseca, Seong, and Burkhardt "Impact of resist blur on MEF, OPC, and CD Control" Proc. of SPIE Vol. 5377 (2004) pp. 141-149

[12] Fuard, Besacier, and Schiavone "Validity of the diffused aerial image model: an assessment based on multiple test cases" Proc. of SPIE Vol. 5040 (2003) pp.1536-1543

[13] Granik, Cobb, and Medvedev "Application of CM0 resist model to OPC and verification" Proc. of SPIE 6154 (2006) 61543E-1

[14] Granik, Medvedev, and Cobb "Toward standard process models for OPC" Proc. of SPIE 6520 (2007) 652043

[15] Zhang, Song, Lucas, and Shiely "Modeling of Focus Blur in the Context of Optical Proximity Correction" Proc. of SPIE 6924 (2008) 69243K